NONLINEAR CONTROLS ON EVAPOTRANSPIRATION IN ARCTIC COASTAL WETLANDS

[1,2]Anna K. Liljedahl, *akliljedahl@alaska.edu*

[1]Larry D. Hinzman, [1,3]Yoshinobu Harazono, [4]Donatella Zona, [5]Craig E. Tweedie, [6]Robert D. Hollister, [7]Ryan Engstrom, and [8]Walter C. Oechel

[1]International Arctic Research Center, University of Alaska Fairbanks, Fairbanks, AK-99775, USA; [2]Water and Environmental Research Center, University of Alaska Fairbanks, Fairbanks, AK-99775, USA; [3]Osaka Prefecture University, Sakai, Osaka-599-8531, Japan ; [4]Research Group of Plant and Vegetation Ecology, University of Antwerp, B-2610 Wilrijk, Belgium; [5]Department of Biology, University of Texas at El Paso, El Paso, TX-79968, USA; [6]Department of Biology, Grand Valley State University, Allendale, MI-49401, USA; [7]Department of Geography, The George Washington University, Washington, DC-20052, USA; [8]Department of Biology, San Diego State University, San Diego, CA-92182, USA

Keywords: Evapotranspiration, Arctic, wetland, energy, ecohydrology

ABSTRACT

Projected increases in air temperature and precipitation due to climate change in Arctic wetlands could dramatically affect ecosystem functioning. As a consequence, it is important to define the controls on evapotranspiration, which is the major pathway of water loss from these systems. We quantified the multi-year controls on midday arctic coastal wetland evapotranspiration measured with the eddy covariance method at two vegetated drained thaw lake basins near Barrow, Alaska. Variations in near-surface soil moisture and atmospheric vapor pressure deficits were found to have nonlinear effects on midday evapotranspiration rates. Vapor pressure deficits near and above 0.3 kPa appeared to be an important hydrological threshold, allowing latent heat fluxes to persistently exceed sensible heat fluxes. Dry compared to wet soils increased the bulk surface resistance (water-limited). Wet soils favored ground heat flux and therefore limited the energy available to sensible and latent heat fluxes (energy-limited). Thus, midday evapotranspiration was suppressed on both dry and wet soils through different mechanisms. We also found that wet soils (ponding excluded) combined with large atmospheric demands resulted in an increased bulk surface resistance and therefore suppressing the evapotranspiration to below its potential rate (Priestley-Taylor $\alpha < 1.26$). This was likely caused by the limited ability of mosses to transfer moisture during large atmospheric demands. Ultimately, in addition to net radiation, the various controlling factors on midday evapotranspiration (near-surface soil moisture, atmospheric vapor pressure, and the limited ability of mosses that are saturated at depth to transfer water during high atmospheric vapor demands) resulted in an average evapotranspiration rate of up to 75 % of the potential evapotranspiration rate. The multiple limitations on midday

evapotranspiration rates have the potential to moderate interannual variation of total evapotranspiration and dampen excessive water loss during a warmer climate. Combined with the prevailing maritime winds and the projected increase in precipitation, these dampening mechanisms will likely prevent extensive future soil drying and hence maintain the presence of coastal wetlands.

1 Introduction

The response of arctic wetland hydrology to projected climate warming is uncertain. Evapotranspiration is the least understood component in the Arctic hydrologic cycle (Kane et al., 1989, 1992; Vörösmarty et al., 2001; Woo et al., 2008). Regional studies have proposed increased (Lafleur, 1993) to unchanged (Rouse et al., 1992) future evapotranspiration rates from arctic coastal wetlands. As evapotranspiration is the major pathway of water loss from the flat tundra landscape (Rovansek et al., 1996; Mendez et al., 1998; Bowling et al., 2003), an increase in evapotranspiration could reduce the extent of arctic wetlands (Barnett et al., 2005). If soil drying occurs the region that for a long time has sequestered carbon will shift to a carbon source causing a positive feedback to global climate warming (Oechel et al., 1998; Olivas et al., 2010).

A vast majority of extremely-low gradient arctic tundra is located within 135 km of the Arctic Ocean (Walker et al., 2005; Minke et al., 2007). The summer climate of the arctic coastal zone is controlled by a steady mesoscale phenomenon; a nearly 24-hour sea breeze (Moritz, 1977; Walsh, 1977; Kozo, 1979, 1982) resulting in low diurnal temperature fluctuations and low atmospheric vapor pressure deficits (VPD). All components of the coastal wetland energy balance, except net radiation, depend on wind direction with cold moist maritime air suppressing evapotranspiration losses (Rouse et al., 1987). One may expect the sea-breeze to continue in a warmer climate, yet the fate of future evapotranspiration rates from coastal wetlands is uncertain.

Measurement of energy fluxes in arctic environments are challenging due to climatic and logistical constraints. Hence, most field studies are of relatively short duration. There are several field studies of arctic surface energy exchange (see Eugster et al., 2000) and arctic water balance (see Kane and Yang, 2004) but few studies have conducted multi-year analyses of evapotranspiration measured by the eddy covariance technique.

Here we present results from one of the longest time series of flux measurements available for any arctic ecosystem represented by two vegetated drained thaw lake basins (5 summers at one site; 3 summers in an adjacent site) on the Arctic Coastal Plain, Alaska. Our objective is to define mechanisms controlling midday evapotranspiration rates from seasonally inundated Arctic coastal wetlands. We hypothesize that the evapotranspiration experience multiple controls apart from surface net radiation. Defining these controls is important in refining our understanding of the future hydrologic regime, Arctic ecosystem changes, and their global implications.

2 Background

Extremely low-relief wetlands represent a significant portion (> 400,000 km^2) of the pan-Arctic landscape (Walker et al., 2005) and are unique in that they exist in an environment with a desert-like annual precipitation (~ 250 mm yr^{-1}). Sparse summer runoff (Brown et al., 1968; Kane et al., 2008) limits the summer net water balance to summer precipitation minus evapotranspiration. A negative summer net water balance is common (Mendez et al., 1998) but it is offset by the annual replenishment of water from snowmelt (Rovansek et al., 1996). The abundance of snowmelt water results in extensive surface inundation during the first week following snowmelt (Bowling et al., 2003; Woo et al., 2006). Spring runoff is not generated until the surface stores are replenished (Rovansek et al., 1996;

Bowling and Lettenmaier, 2010). Accordingly, evapotranspiration is the major pathway of water loss in summer and it also affects the lateral exports of water.

Evapotranspiration from wet and moist tundra ecosystems of the North Slope of Alaska is estimated to be 0.8-4.2 mm day^{-1} resulting in estimated annual totals ranging from 70 to 190 mm (see summary by Vourlitis and Oechel, 1997). A majority of the evapotranspiration is represented by evaporation from moss and open water (55 to 85%) (see review by Engstrom et al., 2006) even though bryophytes receive only 10-20 % of direct solar radiation during a clear summer day (Miller and Tieszen, 1972). Upward migration of water, attributed to capillary flow, has shown to occur with 0.2 m deep water tables in *Sphagnum* moss (Hayward and Clymo, 1982; Price et al., 2009). Capillary water flow in moss, and hence moss evaporation, is negligible at water potentials below –0.1 MPa (Hayward and Clymo, 1982). In comparison, stomatal closure due to water stress by the typical vascular plants occurs at soil water potentials of –0.4 MPa (*Arctophila fulva*) to –1.2 MPa (*Carex aquatilis*) (Stoner and Miller, 1975; Johnson and Caldwell, 1975). Total transpiration is closely related to Leaf Area Index (LAI) as stomatal closure is rare at wet coastal Arctic sites (Miller and Tieszen, 1972). However, plant-scale studies have also shown that the conductance of tundra plants can be reduced by leaf cell water stress induced by vapor pressure gradients ranging from 0.7 to 2 kPa between the leaf and the ambient air (Johnson and Caldwell, 1975). Arctic bryophytes are extremely sensitive to air vapor pressure deficits due to the direct changes in tissue water content (Oechel and Sveinbjörnsson, 1978).

The effect of maritime air mass on surface energy partitioning affect tundra 135 km inland from the Arctic Coast (Harazono et al., 1998). Cold moisture-laden air along the coast increases the partitioning of surface energy into sensible heat flux (*H*) due to a) a steep temperature gradient between the ground surface and air, which favors *H*, and b) a nearly saturated air mass that reduces latent heat flux (*LE*) (Rouse et al., 1987; Lafleur and Rouse, 1988, 1995; Price, 1991; Harazono et al., 1998; Boike et al., 2008). This, at least partly, explains the finding that despite the wet soils evapotranspiration is in general below its potential rate in coastal arctic wetlands (Rouse et al., 1987; Mendez et al., 1998). However, it is unclear what values in air vapor pressure deficits result in significant changes to surface energy partitioning and evapotranspiration rates.

Soil moisture may play a major role on tundra surface energy balance partitioning. The surface energy partitioning shifted from being dominated by latent heat in the early season when water table was near the ground surface to being dominated by sensible heat in late summer when water tables were 30 cm below the ground surface at a coastal wet- and moist herbaceous tundra site (Vourlitis and Oechel, 1997). Further, wet organic soils transfer heat more efficiently than dry organic soils (Farouki, 1981; Hinzman et al., 1991), which in theory, would leave less net radiation available to sensible and latent heat fluxes. That evokes the question whether the arctic wetlands display important controlling mechanisms on the local hydrological system that constrain evapotranspiration rates not only during dry near-surface conditions but also when wet.

3 Site description

The two sites, hereafter referred to as Central Marsh, CM, (71º19'12.5"N, 156º37'20.211"W, elevation 1 m) and the Biocomplexity Experiment, BE, (71°16'51.17"N 156°35'47.28"W, elevation 4.5 m) are located 4.5 km apart, and both are only few kilometers from the ocean near Barrow, Alaska, on the Arctic Coastal Plain (Fig. 1). Mean annual air temperature at Barrow Airport is −12 °C (1977-2009) with a summer (June through August) average of 3.3 °C. A large amount of the annual adjusted precipitation (173 mm, 1977-2009) falls during June through August (72 mm). Fog and drizzle are common during the summer because the area receives a steady cool and moist wind (mean 5 m s^{-1}) off the ocean from east-northeast (Shulski and Wendler, 2007). The BE site is located in the control treatment of a large-scale hydrologic manipulation experiment that began in 2007 (identified as the South site in the work by Zona et al. (2009a)). Unlike the other treatments this site did not have manipulated water tables.

The BE and CM sites are representative of vegetated drained thaw lake basins that appear to have drained between 50 and 300 years ago (Hinkel et al., 2003). The sites are poorly drained and are characterized by wet meadow tundra with Typic Aquiturbels soils (Bockheim et al., 1999) underlain by 600 m thick permafrost (Brown and Johnson, 1965). Low-centered ice-wedge polygons are found at the vegetated drained thaw lake basin while high-centered ice-wedge polygons cover the upland areas of the watersheds. Vegetated drained thaw lake basins (Mackay, 1963) occupy approximately 26 % of the Arctic Coastal Plain (Hinkel et al., 2005) and 50 % of the Barrow Peninsula north of ~71° latitude (Hinkel et al., 2003). Longer-term (>2 yr) energy balance measurements of vegetated drained thaw lakes are limited, which constrains our understanding of interannual controls of evapotranspiration rates from this vast region.

Non-vascular vegetation contributes significantly to biomass and land cover (Webber 1974, 1978; Oechel and Sveinbjornsson, 1978; Rastorfer 1978). Bryophytes represent between 60 and 95 % of the overall live biomass in similar wet meadow communities (Tieszen, 1978) with much of the variation due to small scale heterogeneity associated with micro-topography (Tieszen, 1978; Hollister and Flaherty, 2010). Across the BE drained lake bed, mosses represent most of the live above ground biomass (Zona et al., 2009a,b; 2011). Up to 60 % of the ecosystem net day time CO_2 uptake at the end of the growing season at BE is represented by *Sphagnum* (Zona et al., 2011). Accordingly, controls on evapotranspiration rates from this landscape are likely dominated by moss evaporation processes.

The sites differ somewhat in vascular plant composition, LAI (green biomass unless otherwise stated) and the amount of standing dead biomass (which is defined as attached or upright dead plant matter). *Arctophila fulva* is the dominant vascular plant species at the CM site where vegetation is also represented by sedges, mosses and lichens. LAI at the CM site reached 1.4 in mid-August 2001 (Mano, 2003). Mid-August LAI at the BE vegetated drained lake reached 0.58 in 2006 where the vascular plant coverage is dominated by *Carex aquatilis* (Zona et al., 2011). Sedges at the BE site did not experience water stress in mid-July 2008 (P. Olivas, unpublished data). Standing dead leaf biomass in the Barrow area reaches 1.23 $m^2\ m^{-2}$ (Dennis et al., 1978). The CM site has a larger abundance of standing dead biomass than the BE site (personal observation). End of growing season plant senescence extends from the end of August to late September (Myers and Pitelka, 1979).

The sparseness of live subsurface material at depths greater than 25 cm at Barrow suggests that the cold temperatures near the bottom of the active layer are limiting to vascular root growth (Dennis and Johnson, 1970). Moss may reach thicknesses of 20 cm at wet sites but the bulk of their living biomass is usually within ~1 cm of the soil surface

(Engstrom et al., 2005). While the rate of thaw is higher in early summer, the maximum thaw depth (active layer depth) is reached in late August/September. The active layer depth at a nearby drained lake basin varied from 19 to 62 cm (mean 36 cm) in 1995-2009 while the mean active layer depth at the BE site was 30 cm (2006), and 26 cm (2007 and 2008) (Shiklomanov et al., 2010).

4 Methods

The controls on midday evapotranspiration rates were assessed through surface energy balance partitioning, the McNaughton and Jarvis Ω-factor, and by solving for parameters in the Penman-Monteith and the Priestley-Taylor equations. The results were then analyzed in the context of soil moisture and meteorological conditions.

4.1 Measurements

We collected summer measurements (June through August) for five years at the CM site (1999-2003) and three years at the BE site (2006-2008). Energy flux measurements were made at a 10 Hz sampling interval using an eddy covariance system. The path length of anemometer and gas analyzer sensor at CM was 10 cm and the separation distance between the center of sonic anemometer and open-path IRGA sensors was 16 cm. The three components of wind speed, air temperature and water vapor concentration from the above sensors were recorded on a magneto-optical disc by a digital recorder (Teac, DRM3). At BE, the sensor separation of the Li-7500 and WindMasterPro was 10 cm. The Li-7500 was calibrated every two to four weeks using ultra high purity nitrogen as zero and a dew point generator (Li-610, Li-COR) that produced an air stream with a known water vapor dew point. Micrometeorological variables were sampled on a data logger every 5 s (CM) or 10 s (BE) and then averaged every 30 min. Additional descriptions of the measurements and data analysis are presented in the work of Harazono et al. (2003) and Zona et al. (2009a).

Measurements of the volumetric water content (VWC) at two locations within the CM drained lake basin were obtained in 2000-2003 by inserting a 7 cm Vitel probe (Hydra soil moisture probe, Vitel Inc.) vertically into the ground. The instrument was calibrated through comparison to multiple oven-dried soil samples (Engstrom et al., 2005). The CM site was often inundated in early summer. Such events are here presented as 100 % VWC to indicate ponding.

Hourly atmospheric air pressure for years 1999-2003 were obtained from the NCDC web archive (http://cdo.ncdc.noaa.gov/cgi-bin/cdo/cdostnsearch.pl) and used in the calculations of the psychrometric constant. Long-term records of daily precipitation and air temperature were retrieved from the National Climatic Data Center (NCDC) web archive for the Barrow Airport (STN 700260, WBAN 27502, http://www.ncdc.noaa.gov/cgi-bin/res40.pl?page=gsod.html). The characteristic increase in net radiation defined the start date of the summer.

4.2 Eddy covariance calculations

We calculated fluxes of heat and momentum in 30 min. intervals according to typical covariance calculation procedures. The following corrections were applied (Harazono et al., 2003; Zona et al., 2009a): the humidity effect on the sonic thermometry (Kaimal and Gaynor, 1991), effects of path length and sensor separation on the spectrum for high-frequency flux ranges (Moore, 1986), air density effects (Webb et al., 1980; Leuning et al., 1982), and coordinate rotation (Tanner and Thurtell, 1969). We removed calculated fluxes during rain, fog, and low wind, which may have caused a bias (i.e. reduced representation of low evapotranspiration rates). Extreme amplitudes in the flux data (greater than three times the average) were removed. At the BE site, fluxes of latent heat, sensible heat and momentum were calculated using the EdiRe program and software (version 1.4.3.1169, Robert Clement, University of Edinburgh). No gap filling was performed when analyzing the bulk parameters and energy flux ratios. Midday represented half hourly values around solar noon (defined as ± 2 hours from local solar noon ~ 14:00 Alaska Standard Time). Extreme amplitudes in the bulk parameters (greater than six times the average) were removed. All analyses, except the total daily evapotranspiration, represent non-gap filled midday values. For daily evapotranspiration rates, gap filling was performed for missing data (< 3.5 consecutive hours) using linear interpolation. Negative latent heat fluxes were given a value of zero as the eddy covariance instruments are not designed to measure dew deposition rates. The ending date of the study periods was August 31 although the effective date was dependent upon the available data. The start-date in each year was at its earliest the first day after the snowmelt completion although the effective date depends upon the available data.

4.3 Soil moisture analysis

Unfrozen soil moisture as percent saturation was estimated from volumetric water content measurements at 10 cm depth at the BE site. The spring peak in soil moisture was assumed to represent saturated conditions (100%, all micro and macro pore spaces filled with liquid water). In winter, the organic soil was assumed to have 6 % saturation with unfrozen water content (Hinzman et al., 1991). Soil water potential (ψ) was calculated by fitting a curve after van Genuchten (1980) to a measured water potential sequence (WP4-T, Decagon Devices) from a surface organic moss layer sampled at the BE site. We adjusted the daily precipitation to account for gage undercatch according to Yang et al. (1998).

4.4 Analysis of resistances and equilibrium evaporation

The Penman-Monteith equation (Monteith, 1973) is expressed in terms of aerodynamic, r_a, and bulk surface resistance, r_c:

$$LE = \frac{sQ_a + \frac{\rho C_p [e_s(T_a) - e_a]}{r_a}}{s + \gamma \left[1 + {r_c}/{r_a}\right]} \qquad (1)$$

where s is the slope of the saturation vapor pressure curve versus temperature modified from Brutsaert (1982), Q_a is available energy (W m^{-2}), γ is the psychrometric constant (kPa K^{-1}), ρ the air density (kg m^{-3}); C_p is the specific heat capacity of air (kJ kg^{-1} K^{-1}) at constant pressure, e_s the saturation vapor pressure (kPa) at T_a, which is the ambient air temperature (K), and e_a the air vapor pressure (kPa). Shallow ponded water can represent a significant portion (< 50 %) of the net radiation partitioning (Harazono et al., 1998). Therefore, we defined Q_a as the sum of sensible (H) and latent heat (LE) fluxes since no water temperature measurements were obtained. The aerodynamic resistance, r_a (s m^{-1}), is calculated from Equation (2) following Monteith (1973) with an additional term on the right side representing the laminar boundary layer resistance from Thom (1975) and Lafleur and Rouse (1988):

$$r_a = \frac{u}{u*^2} + \frac{4}{u*} \qquad (2)$$

where $u*$ is friction velocity (m s^{-1}) obtained by eddy covariance measurements and u is wind speed. From here and onwards, the sum of the aerodynamic and laminar boundary layer resistance in Equation 2 is referred to as aerodynamic resistance (r_a). The aerodynamic resistance is the bulk meteorological descriptor of the role of atmospheric turbulence in evaporation.

The isothermal resistance, r_i, (m s^{-1}) was originally defined by Monteith (1965) and is sometimes referred to as the climatological resistance. It is the ratio of water vapor deficit to available energy at the canopy

$$r_i = \frac{\rho \times C_p}{\gamma} \frac{(e_s - e_a)}{Q_a} \qquad (3)$$

(Stewart and Thom, 1973)

Equations (1), (3) and the Bowen ratio, β, which is the ratio of sensible over latent heat, can be combined to solve for the bulk surface resistance, r_c (m s^{-1}):

$$r_c = (1 + \beta) r_i + \left(\beta \frac{s}{\gamma} - 1\right) r_a \qquad (4)$$

The bulk surface resistance characterizes the control of water loss by a vascular plants, non-vascular vegetation, and bare ground.

The bulk surface resistance approaches zero either because the surface boundary layer becomes saturated and VPD = 0 or the air travels over an unsaturated surface with constant r_c and the moisture deficit in the air becomes equal to the value of the surface. A r_c close to 0 results in Penman-Monteith Equation (Monteith, 1973) collapsing into:

$$LE = \alpha\left(\frac{s}{s+\gamma}\right)Q_a \qquad (5) \qquad \text{(Priestley and Taylor, 1972)}$$

which is known as the Priestley-Taylor equation. The evapotranspiration is referred to as "equilibrium" when α equals one, which is most commonly achieved when VPD = 0 (note that equilibrium rates can also be measured over unsaturated surfaces and VPD > 0). The method assumes that the latent heat flux depends only upon the absolute temperature and the available energy. Results from a variety of arctic sites, both wet and dry, indicate that latent heat flux is often above the equilibrium rate (see Engstrom et al., 2002), as originally suggested by Priestley and Taylor (1972) at a non-water-limited grassland. Larger scale mixing of the planetary boundary layer and the entrainment of drier air from above the mixed layer results in evaporation over saturated surfaces greater than the "equilibrium" rate (McNaughton and Jarvis, 1983; DeBruin, 1983). DeBruin (1983) indicates α is a function of wind speed, surface roughness, and bulk surface resistance. Here we defined the potential evapotranspiration by setting the α-value to 1.26 (Priestley and Taylor, 1972).

The McNaughton and Jarvis Ω-factor sets the relative importance of r_c and r_a:

$$\Omega = \left(1 + \frac{s}{s+\gamma}\frac{r_c}{r_a}\right)^{-1} \qquad (6)$$

A vigorous turbulent mixing of the air mass suppresses Ω by promoting increased VPD at the surface. Limited atmospheric mixing results in Ω approaching unity (McNaughton and Jarvis, 1983). However, Ω will approach 0 as long as $r_c >> r_a$. In general, VPD is the main driver of evapotranspiration when Ω is low, while net radiation has the dominant control during Ω near 1.

5 Results

5.1 Meteorological and hydrologic conditions

The analyzed measurements represented the thawed season through August (1999-2003 and 2006-2008). Mean air temperature (Jun.-Aug., 3.2 °C) and precipitation (Jun.-Sep. mm) were near the long-term means (3.4 °C and 99 mm, respectively yr 1979-2008) but large interannual variations occurred (Table 1). Summer 2007 experienced unusually high air temperatures (5.4 °C) and low precipitation (24 mm). Most of the 2007 summer precipitation occurred in a single event in mid-August. During all study periods, 77 % of the daily precipitation rates were less than 2 mm day^{-1}. Trace observations (< 0.13 mm) represented 33 % of all recorded events. Accumulated winter precipitation ranged from 93 to 158 mm of snow water equivalent (SWE).

The maritime nature of both sites lead to low variability in VPD and air temperature. Mean daily VPD was 0.08 kPa with a typical diurnal min and max of 0.02 and 0.17 kPa, respectively. Mean midday VPD was similar amongst all years (0.10-0.13 kPa) except summer of 2007 which was higher (0.17 kPa) (Table 1). The maximum VPD recorded was 1.76 kPa, but days exceeding VPD's of 0.3 kPa were few (8 to 14 days per summer).

Onshore summer winds defined as winds originating from between 1-135 and 225-360 degrees occurred 89 % of the time (1999-2008). Air during onshore winds was colder than the ground surface (Table 2). Offshore winds (from land to sea) typically produced higher VPD's and air temperatures than onshore winds, reversing the typical midday temperature gradient between the air and the ground surface.

The moss surface and organic soils remained close to saturation throughout the study periods with the exception of 2007 (Fig. 2). The soils within the vegetated drained lake basins were unusually dry in late July 2007 (water table dropped below 15 cm depth). Snowmelt water recharged the drained lake soil water storage in spring. Water table measurements at the BE drained lake basin show a multi-week long ponding period following the snowmelt (note that the water table measurements did not capture the start of the inundation). About 10 cm of water accumulated above the ground surface following snowmelt. The drained lake basins also experienced inundation in late summer (2001 and 2008) resulting in an inundation for at least half of the summer's duration. No soil water measurements were made in summer 1999 but the near-normal precipitation (82 mm) suggests wet soil conditions.

5.2 Surface energy exchange

The energy balance closure was not complete (CM 80 % and BE 95 %, Table 3) but comparable to other tundra and grassland ecosystems reported by Eugster et al. (2000) , Wilson et al. (2002) Cava et al. (2008) and Ryu et al. (2008). A major portion of the midday surface energy balance was partitioned into sensible heat flux (CM 35 % and BE

48 %) resulting in a mean midday Bowen ratio above unity at both sites (1.40 at CM and BE). Latent heat flux represented 29 % and 35 % and ground heat flux averaged 16 % and 12 % at CM and BE, respectively. A plot of the seasonal and interannual variations in midday energy partitioning across the thawed season suggest a somewhat consistent partitioning into *LE* (Fig. 3a, b) despite large interannual differences in soil moisture (Fig. 2).

Mean midday evapotranspiration (ET) rates showed large day-to-day variations, which was also found in total daily ET. Measured total evapotranspiration ranged from 0.1 to 4.7 mm day^{-1} (mean 1.5 mm day^{-1}) and 0.2 to 3.4 mm day^{-1} (mean 1.9 mm day^{-1}) at the CM (311 days) and BE (46 days) sites, respectively. The high McNaughton and Jarvis Ω-factor (CM 0.74 and BE 0.75) suggests that net radiation was the main control on evapotranspiration rates. Overall mean midday evapotranspiration was near or below the equilibrium rate (CM 0.94 and BE 0.88) (Table 3). An overall average evapotranspiration rate of 75 % (CM) and 70 % (BE) of the potential rate (α 1.26) indicates additional controls than net radiation.

The effect of soil moisture on Priestley-Taylor α was gradual. Approximately 64 % ($P < 0.01$, probability that correlation is zero) of the variance in the Priestley-Taylor α was correlated to the near-surface soil moisture (Fig. 4a). Focusing on a time period (July 20 through August 12) that displayed unusually dry soils ($\Psi < -0.13$ MPa) in 2007 and that was wet, although not inundated, in the other years provides additional comparisons (Table 4). In addition to decreased Priestley-Taylor α value, the dry soil reduced Ω. Bulk surface resistance also responded to dry (r_c 57 s m^{-1}) and wet soils (41 s m^{-1}) and displayed a statistically significant trend in summer 2003 and 2007. Accordingly, reduced soil moisture had a suppressing effect on ET.

Despite the differences in Priestley-Taylor α and r_c, late-summer partitioning of net radiation into *LE* was strikingly similar between dry and wet soils (37 and 34 %, respectively). This suggests additional controls than bulk surface resistance to ET. Wet soils increased the partitioning to ground heat flux from ~6 % (dry) to 14 % (saturated conditions) (Fig. 4b, Table 4), which resulted in less energy available to midday *LE* and *H*.

VPD affected the energy balance partitioning and the Priestley-Taylor α. Latent heat fluxes from a wet surface were always slightly larger than sensible heat fluxes (Bowen ratios below unity) if VPDs were above 0.25 (2006), 0.31 (2007), and 0.28 kPa (2008) (Fig. 5). A VPD above these thresholds during wet soils (including ponding) resulted in a Priestley-Taylor α near one or higher. On the other hand, unusually dry soil ($\Psi < -0.13$ MPa, July 20 – Aug 12, 2007) resulted in evapotranspiration below the equilibrium rate despite VPD reaching 1.7 kPa. Nevertheless, a VPD > 1.2 kPa resulted in latent heat fluxes exceeding the sensible heat fluxes at dry soils.

A VPD below and above 0.3 kPa resulted in significantly different bulk parameters during wet soils (no ponding) (Table 5). A VPD > 0.3 kPa resulted in a slightly increased Priestley-Taylor α and a doubled r_c while β and Ω was reduced (15 Jul. – 15 Aug. 1999-2003 and 2006). High bulk surface resistance (~100 s m^{-1}) often occurred with elevated VPD throughout the study period (Fig. 6). This suggest that a) net radiation was the primary control on ET from wet soils when VPD < 0.3 kPa and b) that increased bulk surface resistance suppressed the evapotranspiration during large atmospheric demand even if the soils were wet.

The surface energy partitioning depended on wind direction (Table 2). Onshore winds favored energy partitioning into sensible heat flux (β 1.37), while the Bowen ratio was slightly below unity during offshore conditions (0.87) at the CM site. Both the partitioning into ground and latent heat increased with offshore winds, while the sensible heat flux portion decreased. No onshore-offshore analysis was performed at the BE site as the two wind directions represents differing landscape features (drained thaw lake and uplands, respectively).

Two days in late July 2000 show the cascading effects on meteorological conditions and surface energy balance that were induced by altered wind directions (Fig. 7). The first day represent near-normal meteorological conditions with onshore winds resulting in an equal partitioning of *LE* and *H*. Offshore winds occurred during the following day, which resulted in high VPD (1.3 kPa) and *LE* dominating *H*. The *LE* exceeded *H* when the VPD passed 0.37 kPa (see vertical dashed lines). Conversely, *LE* and *H* became equal later in the afternoon when the VPD returned to 0.37 kPa. Bulk surface resistance and Priestley-Taylor α responded accordingly with increasing mean midday bulk surface resistance (from 75 to 128 s m^{-1}) and Priestley-Taylor α (from 0.84 to 1.03).

6 Discussion

Our analyses confirm earlier landscape-scale work from coastal arctic wetlands that relied on Bowen ratio and energy balance techniques as well as plant-scale ecohydrological studies from the Arctic Coastal Plain. The high McNaughton and Jarvis Ω-factor suggests that net radiation was the main control on evapotranspiration rates but our results show that midday evapotranspiration rates are additionally constrained during both wet and dry near-surface conditions. We concur with previous studies that state the importance of maritime air mass favoring sensible heat (large temperature gradients) and suppressing latent heat flux (low VPD) (Rouse et al., 1987; Lafleur and Rouse, 1988; Price, 1991; Harazono et al., 1998). We also show that near-surface soil moisture conditions and VPD express nonlinear effects on midday evapotranspiration. Ultimately, the various controlling factors (net radiation, soil moisture, VPD, and, despite wet near-surface soils, bulk surface resistance during high VPD) reduced the evapotranspiration under a range of meteorological and hydrologic conditions, which has the potential to buffer interannual variation of total evapotranspiration. Midday evapotranspiration rates were on average 70 (BE) and 75 % (CM) of the potential rate as defined by a Priestley-Taylor α value of 1.26.

The generally low vapor pressure deficits (mean midday 0.12 kPa) play an important role in suppressing the evapotranspiration from the arctic coastal wetlands. A VPD near 0.3 kPa appears to represent a threshold during wet near-surface soils (Fig. 5). Above 0.3 kPa, latent heat fluxes always dominated the sensible heat fluxes, and the evapotranspiration rates always remained near or above the equilibrium rate (Fig. 5, Table 5).

Despite large interannual variations in mean summer air temperatures, the number of days exceeding a VPD of 0.3 kPa varied only between 8 (2003) and 14 days (2001). In addition, it was the coldest summer (2001) that had the most days above 0.3 kPa although the two warmest summers (1999 and 2007) trailed closely behind (12 and 13 days, respectively). Hence, warmer mean summer air temperatures do not necessarily mean an increased number of days with VPD's above 0.3 kPa at Arctic coastal wetlands.

An increased atmospheric demand favored the partitioning of net radiation into *LE*, but an increased bulk surface resistance -despite wet soils- prevented evapotranspiration from reaching its potential rate (α ~1.26) (Table 5). The reduction in Ω suggests that VPD increased its role in controlling evapotranspiration when VPD reached above 0.3 kPa. Simultaneously, a VPD > 0.3 kPa more than doubled the bulk surface resistance, which limited any increase in the Priestley-Taylor α. The rate of water movement through moss (capillary forces upwards from the water table) are likely not able to support potential evaporation rates. Our landscape-scale findings agree with earlier plot-scale studies of tundra vascular and non-vascular conductance (inverse of resistance) (Johnson and Caldwell, 1975; Oechel and Sveinbjörnsson, 1978) where the surface cover (despite wet soils) was unable to deliver enough moisture when atmospheric demands were high.

Hence, the evapotranspiration from the two studied vegetated drained lake was suppressed during both low and high VPD's, but through differing mechanisms. The lower VPDs present a direct atmospheric constraint as the air is unable to hold much additional moisture. The high VPD results in an indirect constraint on evapotranspiration rates through an insufficient transfer rate of water through the moss layer that is expressed through an increased bulk surface resistance.

Near-surface soil moisture plays an important role in controlling energy balance in vegetated drained thaw lake basins. The higher Priestley-Taylor α and the lower bulk surface resistances during high near-surface soil moisture presented reduced constraints on evapotranspiration (Fig. 4a, Table 4). However, the linkage between evapotranspiration and soil moisture appears to be more complex since the ratio of latent heat flux to net radiation was similar amongst dry and wet soils during VPD's below 0.3 kPa. The increased partitioning into ground heat flux was during wet compared to dry soils reduced the energy available for midday sensible and latent heat flux – a phenomenon which has also been discussed by McFadden et al. (1998). Not unlike the discussion about the nonlinear controls of VPD on evapotranspiration, we suggest that midday evapotranspiration was suppressed during both dry and wet soils but through differing mechanisms; (a) water-limitations (dry soils) and (b) energy-limitations (wt soils) through an increased partitioning of net radiation into ground heat flux.

The multiple nonlinear controls may moderate the spatial variability in the energy partitioning from different vegetation types. Short-term mid-summer measurements of LE/R_n at tussock, tussock-shrub, shrub and wet sedge tundra ranged from 35 to 42 % (mean 38 %) (McFadden et al., 1998), which is close to our comparison between wet and dry mid-summer conditions (34 – 37 %). It is apparent however that there is quite a large variability in LE/R_n between sites and time periods from a multitude of short-term eddy covariance measurements across the North Slope of Alaska (Eugster et al., 2000). Nevertheless, the values of LE/R_n including other measures presented in this study agrees well with those reported by Harazono et al. (1998), Eugster et al. (2000), and McFadden et al. (1998, 2003) that represent non-shrub coastal sites in arctic Alaska. Accordingly, the details presented in this study are representative of Arctic Coastal Plain (< 135 km from the ocean) even though the energy partitioning (and controls on ET) may show similarities to other locations and large day-to-day variations.

The measurements employed in this study cannot distinguish transpiration from evaporation, but our results can be compared to past findings. Firstly, measured mean ET rates (1.5 and 1.9 mm day^{-1}) were more than twice as high as the maximum vascular transpiration (0.2 mm day^{-1}) estimated by Miller and Tieszen (1972) during peak LAI. Secondly, the measured near-surface soil water potentials never reached the soil water potentials for stomatal closure typical for tundra vascular vegetation, which value was established by Stoner and Miller (1975) and Johnson and Caldwell (1975). However, soil water potentials surpassed the limit for effective water transport through moss (−0.1 MPa) in July 2007, which simultaneously saw an increased canopy resistance. Had the vascular vegetation played a dominant role, the observed increase in bulk surface resistance in late summer of 2003 and 2007 would have been less likely. This because the soil water potential initiating stomata closure was never reached. In addition, as mosses represent the majority of the live biomass (Zona et al., 2011), one could argue that they represent a key hydrologic pathway between land and atmospheric systems. And, in fact, boreal mosses are known to act as a heat and moisture “rectifier” allowing heat and moisture fluxes to proceed when they are moist and reducing heat and moisture fluxes under hot dry conditions when the uppermost moss surfaces dry (Oechel and Van Cleve, 1986). However, a determination of the amount of transpiration and evaporation on total evapotranspiration would require hydrologic model simulations or isotopic analyses, which are beyond the scope of this study.

Overall, the two vegetated drained thaw lake basins experienced similar distribution in the energy balance partitioning and bulk parameters despite differences in weather amongst the years (Table 1, 3). It should be noted that at least a third of the data from the BE site represents the unusually low precipitation and warm summer of 2007, which may explain differences in site averages. Still, the general partitioning of the energy balance components were similar and even so under a relatively wide range of soil moisture conditions. The limited differences between the two sites and the agreement with previous studies suggest that our findings are representative of the larger arctic coastal wetland domain.

6.1 Future projections

According to global climate model projections for the mid-21st century, summer air temperature and precipitation will generally increase in the Arctic (Walsh, 2008). Some parts of the land-ocean-atmosphere system are projected to change, but we may also hypothesize resistance in some components of the system. For example, future summer air mass conditions at the Arctic Coastal Plain are likely to continue to be dominated by a 24-hour sea breeze, which brings in moist cool air that suppresses the evapotranspiration in addition to the nonlinear controls by soil moisture. The future evapotranspiration rates may therefore remain dampened, which is in agreement with Rouse et al. (1992), while in contradiction to the hypothesis of Lafleur (1993).

However, it is challenging to predict long-term effects of climate warming on arctic coastal wetland hydrology. The integrated response of the coupled permafrost-vegetation-hydrology system to a warmer climate could drastically affect the surface energy exchange by dampening or accelerating the hydrologic fluxes. The presented results offer an example of this complex system as evapotranspiration rates integrated across a common landscape type respond nonlinearly to a multitude of controlling factors.

7 Conclusion

Evapotranspiration from low-relief vegetated drained thaw lake basins experience multiple limitations through nonlinear relationships to atmospheric vapor demand and near-surface soil moisture. We estimated that current midday evapotranspiration rates represent on average < 75 % of the potential rates despite the typical saturated near-surface conditions. Midday evapotranspiration was suppressed through different mechanisms: a) Vapor pressure deficits near and above 0.3 kPa appeared to be an important hydrological threshold, allowing latent heat fluxes to persistently exceed sensible heat fluxes; b) dry compared to wet soils increased the bulk surface resistance (water-limited); c) wet soils favored ground heat flux and therefore limited the energy available to sensible and latent heat fluxes (energy-limited); and d) wet soils (ponding excluded) combined with large atmospheric demands resulted in an increased bulk surface resistance and therefore suppressing the evapotranspiration to below its potential rate (Priestley-Taylor α < 1.26). The latter was likely caused by the limited ability of mosses to transfer moisture during large atmospheric demands. Our landscape-scale analyses agree well with plant-scale ecohydrological studies from the Arctic Coastal Plain. In other words, there is a resistance in the hydrologic system that dampens soil drying of coastal arctic wetlands. We propose that the wetness of the arctic coastal wetlands will persist despite a warming climate due to the prevailing maritime winds, increased precipitation, and multiple controls on evapotranspiration. Refined projections of future evapotranspiration should also include linkages to geomorphology and vegetation dynamics, which was beyond the scope of this study.

8 Acknowledgements

We thank Chapin III, F. S., Eugster, W., and Fox Jr., J. D., for their reviews of early versions of the manuscript. Thanks to Aquierra, A., who provided Figure 1, Busey, R., for technical assistance, and Victorino, G., Villareal, S., and Vargas, S., for assistance with field work, Barrow Arctic Science Consortium for logistical assistance and Ukpeagvik Iñupiat Corporation for land access to the Barrow Environmental Observatory. Financial support for this research was provided through the National Science Foundation, grants 0652838, 0632263, and 0421588. Any opinions, findings, conclusions, or recommendations expressed are those of the authors and do not necessarily reflect the views of NSF. Mention of specific product names does not constitute endorsement by NSF.

9 References

Barnett, T. P., Adam, J. C., and Lettenmaier, D. P.: Potential impacts of a warming climate on water availability in snow-dominated regions, Nature, 438, 303–309, doi:10.1038/nature04141, 2005.

Bockheim, J. G., Everett, L. R., Hinkel, K. M., Nelson, F. E., and Brown, J.: Soil organic carbon storage and distribution in arctic tundra, Barrow, Alaska, Soil Sci. Soc. Am. J., 63, 934–940, 1999.

Boike, J., Wile, C., and Abniozva, A.: Climatology and summer energy and water balance of polygonal tundra in the Lena River Delta, Siberia, J. Geophys. Res., 113, G03025, doi:10.1029/2007JG000450, 2008.

Bowling, L. C. and Lettenmaier, D. P.: Modeling the effects of lakes and wetlands on the water balance of arctic environments, J. Hydrometeorol., 11(2), 276–295, 2010.

Bowling, L. C., Kane, D. L., Gieck, R. E., Hinzman, L. D., and Lettenmaier, D. P.: The role of surface storage in a low-gradient Arctic watershed, Water Resour. Res., 39(4), 1087, doi:10.1029/2002WR001466, 2003.

Brown, J. and Johnson, P. L.: Pedo-ecological investigations at Barrow, Alaska, U.S. Army Cold Regions Research and Engineering Lab., Hanover, USA, Tech. Rep., 159:32, 32 pp., 1965.

Brown, J. R., Dingman, S. L., and Lewellen, R. I.: Hydrology of a drainage basin on the Alaskan Coastal Plain, U.S. Army Cold Regions Research and Engineering Lab., Hanover, USA, Res. Rep. 240, 18 pp., 1968.

Brutsaert, W.: Evaporation into the atmosphere, reprinted 1991, Kluwer Academic Publishers, Dordrecht, The Netherlands, 299 pp., 1982.

Cava, D., Contini, D., Donateo, A., and Martano P.: Analysis of short-term closure of the surface energy balance above short vegetation, Agr. Forest Meteorol., 148, 82–93, 2008.

DeBruin, H. A. R.: A model for the Priestley-Taylor parameter α, J. Clim. Appl. Meteorol., 22, 572–578, 1983.

Dennis, J. G. and Johnson, P. L.: Shoot and rhizome-root standing crops of tundra vegetation at Barrow, Alaska, Arctic Alpine Res., 2(4), 253–266, 1970.

Dennis, J. G., Tieszen, L. L., and Vetter, M. A.: Seasonal dynamics of above- and below-ground production of vacular plants at Barrow, Alaska, in: Vegetation and production ecology of an Alaska Arctic tundra, edited by Tieszen, L. L., Springer-Verlag, New York, pp. 113–140, 1978.

Engstrom, R., Hope, A. Stow, D. A., Vourlitis, G. L., and Oechel, W. C.: Priestley-Taylor coefficient: Variability and relationship to NDVI in arctic tundra landscapes, J. Am. Water Resour. As., 38(6), 1647–1659, 2002.

Engstrom, R., Hope, A., Kwon, H., Stow, D., and Zamolodchikov, D.: Spatial distribution of near surface soil moisture and its relationship to microtopography in the Alaskan Arctic coastal plain, Nord Hydrol., 36(3), 219–234, 2005.

Engstrom, R., Hope, A., Kwon, H., Harazono, Y., Mano, M., and Oechel, W. C.: Modeling evapotranspiration in Arctic coastal plain ecosystems using a modified BIOME-BGC model, J. Geophys. Res., 111, G02021, doi:10.1029/2005JG000102, 2006.

Eugster, W., Rouse, W., Pielke, R. A., McFadden, J. P., Baldocchi, D. D., Kittel, T. G. F., Chapin III, F. S., Liston, G. E., Vidale, P. L., Vaganov, E., and Chambers, S.: Land-atmosphere energy exchange in Arctic tundra and boreal forest: Available data and feedbacks to climate, Glob. Ch. Biol., 6, 84–115, 2000.

Farouki, O. T.: Thermal properties of soil, U.S. Army Cold Regions Research and Engineering Lab., Hanover, N.H., Report 81-1, 1981.

Harazono, Y., Yoshimoto, M., Mano, M., Vourlitis, G. L., and Oechel, W. C.: Characteristics of energy and water budgets over wet sedge and tussock tundra ecosystems at North Slope Alaska, Hydrol. Process., 12, 2163–2183, 1998.

Harazono, Y., Mano, M., Miyata, A., Zulueta, R. C., and Oechel, W. C.: Inter-annual carbon dioxide uptake of a wet sedge tundra ecosystem in the Arctic, Tellus, 55B, 215–231, 2003.

Hayward, P. M. and Clymo, R. S.: Profiles of water-content and pore-size in Sphagnum and peat, and their relation to peat bog ecology, Royal Soc. London Series B – Biol. Sci. Conf. Proceed., 215(1200), 299–325, 1982.

Hinkel, K. M., Eisner, W. R., Bockheim, J. G., Nelson, F. E., Peterson, K. M., and Dai, X.: Spatial extent, age, and carbon stocks in drained thaw lake basins on the Barrow Peninsula, Alaska, Arct. Antarct. Alp. Res., 35, 291–300, 2003.

Hinkel, K. M., Frohn, R. C., Nelson, F. E., Eisner, W. R., and Beck, R. A.: Morphometric and spatial analysis of thaw lakes and drained lake basins in the western Arctic Coastal Plain, Alaska, Permafrost Periglaci., 16, 327–341, 2005.

Hinzman, L. D., Kane, D. L., Gieck, R. E., and Everett, K. R.: Hydrological and thermal properties of the active layer in the Alaskan Arctic, Cold Reg. Sci. Technol., 19, 95–110, 1991.

Hollister, R. D. and Flaherty, K. J.: Above- and below-ground plant biomass response to experimental warming in northern Alaska, Appl. Veg. Sci., 1–10, doi: 10.1111/j.1654-109X.2010.01079.x, 2010.

Johnson, D. A. and Caldwell, M. M.: Gas exchange of four Arctic and Alpine tundra plant species in relation to atmospheric and soil moisture stress, Oecologia, 21, 93–108, 1975.

Kaimal, J. C. and Gaynor, J. E.: Another look at sonic thermometry, Bound.-Lay. Meteorol., 56, 401–410, 1991.

Kane, D. L. and Yang, D.: Overview of water balance determinations for high latitude watersheds, in: Northern Research Basins Water Balance, edited by D. L. Kane and D. Yang, IAHS, Oxfordshire, UK., 1–12, 2004.

Kane, D. L., Hinzman, L. D., Benson, C. S., and Everett, K. R.: Hydrology of Imnavait Creek, an arctic watershed, Holarctic Ecol., 12, 262–269, 1989.

Kane, D. L., Hinzman, L. D., Woo, M-K., and Everett, K. R.: Arctic hydrology and climate change, in: Arctic Ecosystem in a Changing Climate, edited by F. S. Chapin III, R. L. Jeffries, J. E. Reynolds, G. R. Shaver, and J. Svoboda, Academic, San Diego, CA., pp. 35–57, 1992.

Kane, D. L., Gieck, R. E., and Hinzman, L. D.: Water balance for a low-gradient watershed in Northern Alaska, in: Proceedings of the Ninth International Conference on Permafrost, edited by Kane, D. L and Hinkel, K. M., University of Alaska Fairbanks, AK., 883–888, 2008.

Kozo, T. L.: Evidence for sea breezes on the Alaskan Beaufort Sea coast, Geophys Res. Lett., 6, 849–852, 1979.

Kozo, T. L.: An observational study of sea breezes along the Alaskan Beaufort Sea coast: Part 1, J. Appl. Meteorol., 21(7), 891–905, 1982.

Lafleur, P. M.: Potential water balance response to climatic warming: The case of a coastal wetland ecosystem of the James Bay lowland, Wetlands, 13(4), 270–276, 1993.

Lafleur, P. M. and Rouse W. R.: The influence of surface cover and climate on energy partitioning and evaporation in a subarctic wetland, Bound.-Lay. Meteorol., 44, 327–347, 1988.

Lafleur, P. M. and Rouse, W. R.: Energy partitioning at treeline forest and tundra sites and its sensitivity to climate change, Atmos. Ocean, 33, 121–133, 1995.

Leuning, R., Ohtaki, E., Denmead, O. T., and Lang, A. R. G.: Effects of heat and water vapor transport on eddy covariance measurement of CO_2 fluxes, Bound.-Lay. Meteorol., 23, 209–222, 1982.

Mackay, J. R.: The Mackenzie Delta area, N. W. T., Department of Mines and Technical Surveys, Ottawa, Canada, Geographical Branch Memoir 8, 202 pp., 1963.

Mano, M.: Study on the budget of carbon dioxide and methane at an arctic coastal wet sedge tundra (in Japanese), Ph.D. thesis, Chiba Univ., Chiba, Japan, 2003.

McFadden, J. P. and Chapin III, F. S.: Subgrid-scale variability in the surface energy balance of arctic tundra, J. Geophy. Res., 103(D22), 28947 – 28961.

McFadden, J. P., Eugster. W. and Chapin III, F. S.: A regional study of the controls on water vapor and carbon exchange in arctic tundra, Ecol., 84(10), 2762 – 2776.

McNaughton, K. and Jarvis, P. G.: Predicting effects of vegetation changes on transpiration and evaporation, in: Water deficits and plant growth, Vol. VII, edited by Koslowski, T. T., Academic Press, NY., 1–47, 1983.

Mendez, J., Hinzman, L. D., and Kane, D. L.: Evapotranspiration from a wetland complex on the Arctic Coastal Plain of Alaska, Nord. Hydrol., 29(4/5), 303–330, 1998.

Miller, P. C. and Tieszen, L.: A preliminary model of processes affecting primary production in the Arctic tundra, Arctic Alpine Res., 4(1), 1–18, 1972.

Minke, M., Donner, N., Karpov, N., De Klerk, P., and Joosten, H.: Distribution, diversity, development and dynamics of polygons mires: Examples from Northeast Yakutia (Siberia), Peatlands Int., 1, 36–40, 2007.

Monteith, J. L.: Evaporation and the environment, Symp. Soc. Exp. Biol., 19, 205–234, 1965.

Monteith, J. L.: Principles of Environmental Physics, Edward Arnold, London, 1973.

Moore, C. J.: Frequency response corrections for eddy correlation system, Bound.-Lay. Meteorol., 37, 17–35, 1986.

Moritz, R. E.: On a possible sea-breeze circulation near Barrow, Alaska, Arctic Alpine Res., 9(4), 427–431, 1977.

Myers, J. P. and Pitelka F. A.: Variations in summer temperature patterns near Barrow, Alaska: Analysis and ecological interpretation, Arctic Alpine Res., 11, 131–144, 1979.

Oechel, W. C. and Sveinbjörnsson, B.: Photosynthesis of Arctic Bryophytes, in: Vegetation and Production Ecology of an Alaskan Arctic Tundra, edited by Tieszen, L.L., Springer-Verlag, NY., 1978.

Oechel, W. C. and van Cleve, K.: The role of bryophytes in nutrient cycling in the taiga, in: Forest ecosystems in the Alaskan taiga: A synthesis of structure and function, edited by van Cleve, K., Chapin III, F. S., Flanagan, P. W., Viereck, L. A., and Dyrness, C. T., Springer-Verlag, NY., 121–137, 1986.

Oechel, W. C., Vourlitis, G. L., Hastings, S. J., Ault, R. P., and Bryant, P.: The effects of water table manipulation and elevated temperature on the net CO_2 flux of wet sedge tundra ecosystems, Glob. Ch. Biol., 4, 77–90, 1998.

Olivas, P. C., Oberbauer, S. F., Tweedie, C. E., Oechel, W. C., and Kuchy, A.: Responses of CO_2 flux components of Alaskan Coastal Plain tundra to shifts in water table, J. Geophys. Res., 115, G00I05, doi:10.1029/2009JG001254, 2010.

Price, J., Evaporation from a blanket bog in a foggy coastal environment, Bound.-Lay. Meteorol., 57, 391–406, 1991.

Price, J., Edwards, T. W. D., Yi, Y., and Whittington, P. N.: Physical and isotopic characterization of evaporation from Sphagnum moss, J. Hydrol., 369, 175–182, 2009.

Priestley, C. H. B. and Taylor, R. J.: On the assessment of surface heat flux and evaporation using large-scale parameters, Mon. Weather Rev., 100(2), 81–92, 1972.

Rastorfer, J. R.: Composition and bryomass of the moss layers of two wet-tundra-meadow communities near Barrow, Alaska, in: Vegetation and Production Ecology of an Alaskan Arctic Tundra, edited by Tieszen, L.L., Springer-Verlag, NY., 169–184, 1978.

Rouse, W. R., Hardill, S. G., and Lafleur, P.: The energy balance in the coastal environment of James and Hudson Bay during the growing season, J. Climatol., 7, 165–179, 1987.

Rouse, W. R., Carlson, D. W., and Wieck, E. J.: Impacts of summer warming on the energy and water balance of wetland tundra, Climatic Ch., 22, 305–326, 1992.

Rovansek, R. J., Hinzman, L. D., and Kane, D. L.: Hydrology of a tundra wetland complex on the Alaskan Arctic Coastal Plain, U.S.A., Arctic Alpine Res., 28(3), 311–317, 1996.

Ryu, Y., Baldocchi, D. D., Ma, S., and Hehn, T.: Interannual variability of evapotranspiration and energy exchange over an annual grassland in California, J. Geophys. Res., 113, D09104, doi:10.1029/2007JD009263, 2008.

Shiklomanov, N. I., Streletskiy, D. A., Nelson, F. E., Hollister, R. D., Romanovsky, V. E., Tweedie, C. E, and Brown, J.: Decadal variations of active-layer thickness in moisture-controlled landscapes, Barrow, Alaska, J. Geophys. Res., 115, G00I04, doi:10.1029/2009JG001248, 2010.

Shulski, M. and Wendler, G.: Climate of Alaska, University of Alaska Press, Fairbanks, AK., 216 pp., 2007.

Stewart, J. B. and Thom, A. S.: Energy budget in pine forest, Q. J. Roy. Meteor. Soc., 99, 154–170, 1973.

Stoner, W. A. and Miller, P. C.: Water relations of plant species in the wet coastal tundra at Barrow, Alaska, Arctic Alpine Res., 7(2), 109–124, 1975.

Tanner, C. B., and Thurtell, G. W.: Anemoclinometer measurements of Reynolds stress and heat transport in the atmospheric surface layer, University of Wisconsin, USA., [Available from US Army Electronic Command, Atmospheric Sciences Laboratory, Ft. Huachuca, AZ 85613.], Tech Rep. ECOM-66-G22-F, 82 pp., 1969.

Thom, A. S.: Momentum, mass, and heat exchange of plant communities, in: Vegetation and the Atmosphere Vol. 1, edited by Monteith, J. L., Academic Press, NY., 57–110, 1975.

Tieszen, L. L.: Vegetation and production ecology of an Alaskan Arctic tundra, Ecological Studies, Springer-Verlag, New York, NY., 1978.

van Genuchten, M. T. A.: Closed-form equation for predicting the hydraulic conductivity of unsaturated soils, Soil Sci. Soc. Am. J., 44(5), 892–898, 1980.

Vörösmarty, C. J., Hinzman, L. D., Peterson, B. J., Bromwich, D. H., Hamilton, L. C., Morison, J., Romanovsky, V. E., Sturm, M., and Webb, R. S.: The hydrologic cycle and its role in Arctic and global environmental change: A rational and strategy for synthesis study, Arctic Res. Consortium of the U. S., Fairbanks, AK., Report, 84 pp., 2001.

Vourlitis, G. L. and Oechel, W. C.: Landscape scale CO_2, H_2O vapor and energy flux of moist-wet coastal tundra ecosystem over two growing seasons, J. Ecol., 85, 575–590, 1997.

Walker, D. A., Raynolds, M. K., Daniels, F. J. A., Einarsson, E., Elvebakk, A., Gould, W. A., Katenin, A. E., Skholod, S. S., Markon, C. J., Evgeny, S., Moskalenko, N. G., Talbot, S. S., and Yurtsev, B. A.: The circumpolar arctic vegetation map, J. Veg. Sci., 16, 267–282, 2005.

Walsh, J. E.: Measurement of the temperature, wind, and moisture distribution across the northern coast of Alaska, Arctic Alpine Res., 9, 175–182, 1977.

Walsh, J. E.: Climate of the Arctic Marine Environment, Ecol. Appl., 18(2), 3–22, 110, 2008.

Webb, E. K., Pearman, G. I., and Leuning, R.: Correction of flux measurements for density effects due to heat and water vapor transfer, Q. J. Roy. Meteor. Soc. 106, 85–100, 1980.

Webber, P. J.: Tundra primary productivity, in: Arctic and Alpine Environments, edited by Ives, J. D. and Barry, R. G., Methuen, London, UK., 445–473, 1974.

Webber, P. J.: Spatial and temporal variation of the vegetation and its productivity, in: Vegetation and Production Ecology of an Alaskan Arctic Tundra, edited by Tieszen L. L., Springer-Verlag, NY., 37–112, 1978.

Wilson, K., Goldstein, A., Falge, E., Aubinet, M., Baldocchi, D., Berbigier, P., Berndorfer, C., Ceulemans, R., Dolman, H., Field, C., Grelle, A., Ibrom, A., Law, B. E., Kowalski, A., Meyers, T., Moncrieff, J., Monson, R., Oechel, W., Tenhunen, J., Valentini, R., and Verma, S.: Energy balance closure at FLUXNET sites, Agr. Forest Meteorol., 113, 223–243, 2002.

Woo, M.-K., Young, K. L., and Brown, L.: High-Arctic patchy wetlands: Hydrologic variability and their sustainability, Phys. Geogr., 27, 4, 297–307, 2006.

Woo, M. K., Kane, D. L., Carey, S. K., and Yang, D.: Progress in permafrost hydrology in the new millennium, Permafrost Periglac. 19, 237–254, 2008.

Yang, D., Goodison, B. E., Ishida, S., and Benson, C.: Adjustment of daily precipitation data of 10 climate stations in Alaska: Applications of world meteorological organization intercomparison results, Water Resour. Res., 34(2), 241–256, 1998.

Zona, D., Oechel, W. C., Kochendorfer, J., Paw U, K. T., Salyuk, A. N., Olivas, P. C., Oberbauer, S. F., and Lipson, D.: Methane fluxes during the initiation of a large-scale water able manipulation experiment in the Alaskan Arctic tundra, Glob. Biogeochem. Cycles, 23, GB2013, doi:10.1029/2009GB003487, 2009a.

Zona, D., Oechel, W. C., Peterson, K. M., Clements, R. J., Paw, K. T., and Ustin, S. L.: Characterization of the carbon fluxes of a vegetated drained lake basin chronosequence on the Alaskan Arctic Coastal Plain, Glob. Ch. Biol., doi:10:1111/j.1365-2486.2009.02107.x, 2009b.

Zona, D., Oechel, W. C., Richards, J. H., Hastings, S., Kopetz, I., Ikawa, H., and Oberbauer, S.: Light stress avoidance mechanisms in Sphagnum dominated wet coastal Arctic tundra ecosystem in Alaska, Ecology, 9(93), 633–644, 2011.

TABLE 1

Meteorological conditions during the study period (1999-2008) including Snow Water Equivalent (SWE) prior to snowmelt, total precipitation from June through September, mean air temperature June through August, mean midday (12:00 through 16:00) air vapor pressure deficit (VPD), and the number of days that experienced a VPD above 0.3 kPa. Mean precipitation and air temperature 1999-2008 (86 mm and 3.2°C, respectively) were near the long-term (1979-2008) conditions of 99 mm and 3.4 °C, respectively. The end of the study period was August 31st (Julian day 242).

	1999	**2000**	**2001**	**2002**	**2003**	**2006**	**2007**	**2008**	**Mean**
SWE (mm)	122	113	123	93	95	137	98	158	117
Precipitation, Jun.-Sep. (mm)	82	128	124	114	72	72	24	68	86
Mean air temperature, Jun.-Aug. (°C)	4.2	3.1	2.1	2.3	2.5	2.9	5.4	3.3	3.2
Mean midday VPD, Jun.-Aug. (kPa)	0.12	0.13	0.1	0.12	0.12	0.11	0.17	0.12	0.12
VPD > 0.3 kPa, Jun.-Aug. (days)	12	10	14	9	8	10	13	10	11
Start study period (Julian-Day)	163	163	164	156	158	162	162	169	n/a

TABLE 2

Differences in midday (12:00 through 16:00) energy balance partitioning, bulk parameters and air conditions during offshore (from land to ocean) and onshore (from ocean to land) winds at the CM site during the thawed season 1999-2003. The temperature gradient (ΔT) represents the air minus the ground surface temperature (sensor located at 1 cm depth).

	Offshore	**Onshore**
LE/R_n	0.41	0.29
H/R_n	0.22	0.35
G/R_n	0.22	0.15
β	0.87	1.37
α	1.08	0.95
ΔT (°C)	2.33	-1.30
VPD (kPa)	0.21	0.12

TABLE 3

Mean midday (12:00 through 16:00) energy balance partitioning and bulk parameters at the CM (1999-2003) and BE (2006-2008) sites during the thawed season (through August).

	Central Marsh	**Biocomplexity Experiment**
LE/R_n	0.29±0.15	0.35±0.07
H/R_n	0.35±0.14	0.48±0.12
G/R_n	0.16±0.07	0.12±0.05
Closure	0.80±0.23	0.95±0.13
β	1.40±0.67	1.40±0.39
Ω	0.74±0.22	0.75±0.17
α	0.94±0.22	0.88±0.15
r_c (s m^{-1})	46±40	46±38
r_a (s m^{-1})	62±38	63±27
r_i (s m^{-1})	14±14	12±12

Closure = $(LE+H+G)/R_n$

TABLE 4

Mean midday energy partitioning and bulk parameters at the BE site between July 20 and August 12 during wet but not inundated (yrs 2006 and 2008) and dry (yr 2007) soil moisture conditions. Only days with VPD below 0.3 kPa are included. Dry soil moisture conditions represent $\Psi < -0.13$ MPa at 10 cm depth, which equals a water table at ~ 15 cm depth, and no prior precipitation.

	Wet	**Dry**
LE/R_n	0.34±0.08	0.37±0.04
H/R_n	0.43±0.10	0.65±0.06
G/R_n	0.14±0.04	0.06±0.02
Closure	0.91±0.14	1.08±0.08
β	1.33±0.32	1.79±0.25
Ω	0.76±0.08	0.63±0.04
α	0.89±0.09	0.72±0.06
r_c (s m^{-1})	41±22	57±14
r_a (s m^{-1})	63±19	48±10
r_i (s m^{-1})	10±6	7±6

Closure = $(LE+H+G)/R_n$
Dry = $\Psi < -0.13$ MPa

TABLE 5

Average midday energy balance partitioning and bulk parameters during VPD below and above 0.3 kPa at the CM (1999-2003) and BE (2006) site during wet but not inundated near-surface soil moisture conditions (July 15 – August 15).

	Wet Soils	
	VPD < 0.3 kPa	**VPD > 0.3 kPa**
LE/R_n	0.30±0.14	0.36±0.14
H/R_n	0.38±0.16	0.35±0.14
G/R_n	0.15±0.08	0.14±0.07
Closure	0.83±0.21	0.83±0.19
B	1.45±0.61	1.04±0.53
Ω	0.72±0.22	0.59±0.17
α	0.89±0.20	0.91±0.25
r_c (s m^{-1})	51±47	114±61
r_a (s m^{-1})	63±45	64±42
r_i (s m^{-1})	13±12	39±24

Wet soils = Ψ >> –0.13 MPa

FIGURE 1

The Central Marsh (CM) and the Biocomplexity Experiment (BE) sites are located at separate vegetated drained thaw lake basins within 3 kilometers from the ocean outside the town of Barrow, Northern Alaska.

FIGURE 2

The soil water status during the study period (no measurements from 1999) at the CM site (a) and the BE site (b and c). Figure a and b represents multiple locations across the vegetated drained lake basins, while figure c is a continuous record of volumetric soil water content measurements at 10 cm depth near the BE eddy covariance tower converted into % saturation.

FIGURE 3a

The variation in the mean midday energy balance partitioning and evapotranspiration rates during summer 1999-2003 at the Central Marsh site.

FIGURE 3b

The variation in the mean midday energy balance partitioning and evapotranspiration rates during summer 2006-2008 at the Biocomplexity Experiment site.

FIGURE 4

The rate of evapotranspiration in relation to a) the equilibrium rate (Priestley-Taylor α) and b) near-surface soil moisture at the BE site. The partitioning of net radiation, R_n, into ground heat flux is linearly correlated to near-surface soil moisture (10 cm depth). The results represents mean midday values at the BE site.

FIGURE 5

The relationship between mean hourly air vapor pressure deficit (VPD) and a) Bowen ratio (β) or b) Priestley-Taylor α during differing soil moisture conditions at the BE site 2006-2008. Dry soils represent a soil water potential < -0.13 MPa at 10 cm depth. The vertical dashed lines represent the identified critical value of VPD. VPD's above this threshold resulted in a $\beta < 1$ and a Priestley-Taylor α near or above 1. The identified VPD-thresholds were 0.25 (2006), 0.31 (2007), and 0.28 kPa (2008) for wet soils and 1.19 kPa for dry soils (2007).

FIGURE 6

Mean midday values of bulk surface resistance (r_c) and VPD at the CM (4a-e) and BE (4f-h) sites.

FIGURE 7

Meteorological conditions, energy balance, and bulk parameters during a two-day time period (July 22nd and 23rd, 2000) when the wind shifted from onshore to offshore. The high VPD on July 23rd coincides with offshore winds. Latent heat became the dominant heat sink when air vapor pressure deficit reached above 0.3 kPa.

FIGURE 1

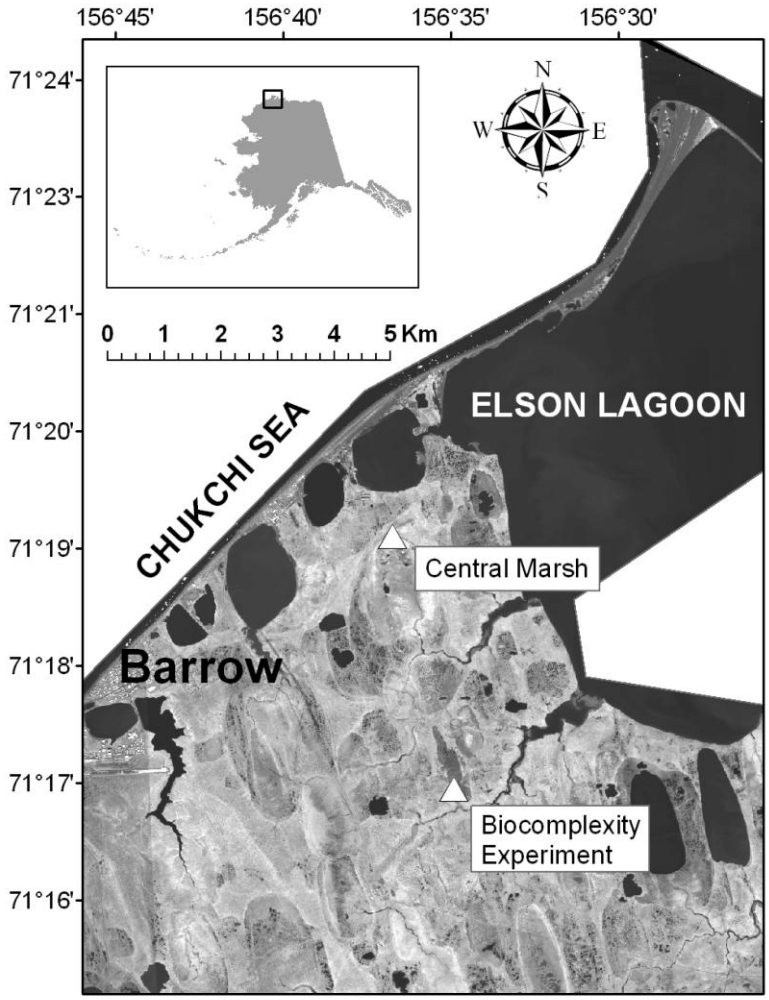
156°45'
156°40'
156°35'
156°30'
71°24'
71°23'
71°21'
71°20'
71°19'
71°18'
71°17'
71°16'
N
W
E
S
0 1 2 3 4 5 Km
ELSON LAGOON
CHUKCHI SEA
Central Marsh
Barrow
Biocomplexity
Experiment

FIGURE 2

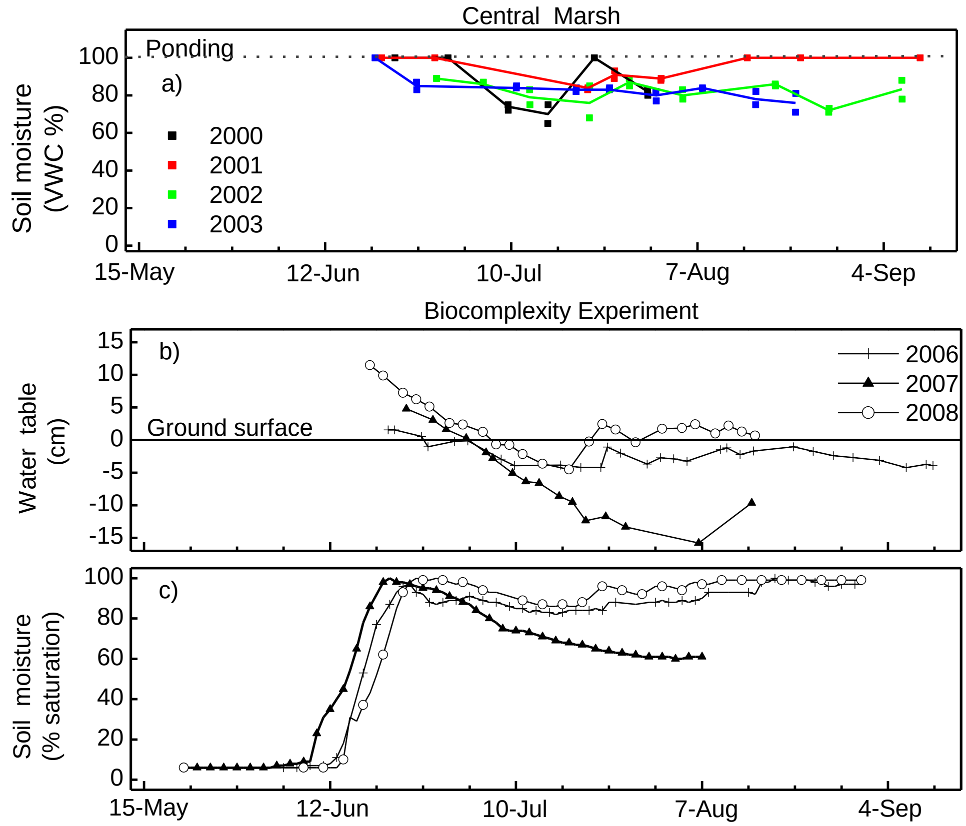

Central Marsh
Ponding
a)
2000
2001
2002
2003
Soil moisture (VWC %)
100
80
60
40
20
0
15-May
12-Jun
10-Jul
7-Aug
4-Sep
Biocomplexity Experiment
b)
2006
2007
2008
Ground surface
Water table (cm)
15
10
5
0
-5
-10
-15
c)
Soil moisture (% saturation)
100
80
60
40
20
0
15-May
12-Jun
10-Jul
7-Aug
4-Sep

FIGURE 3a

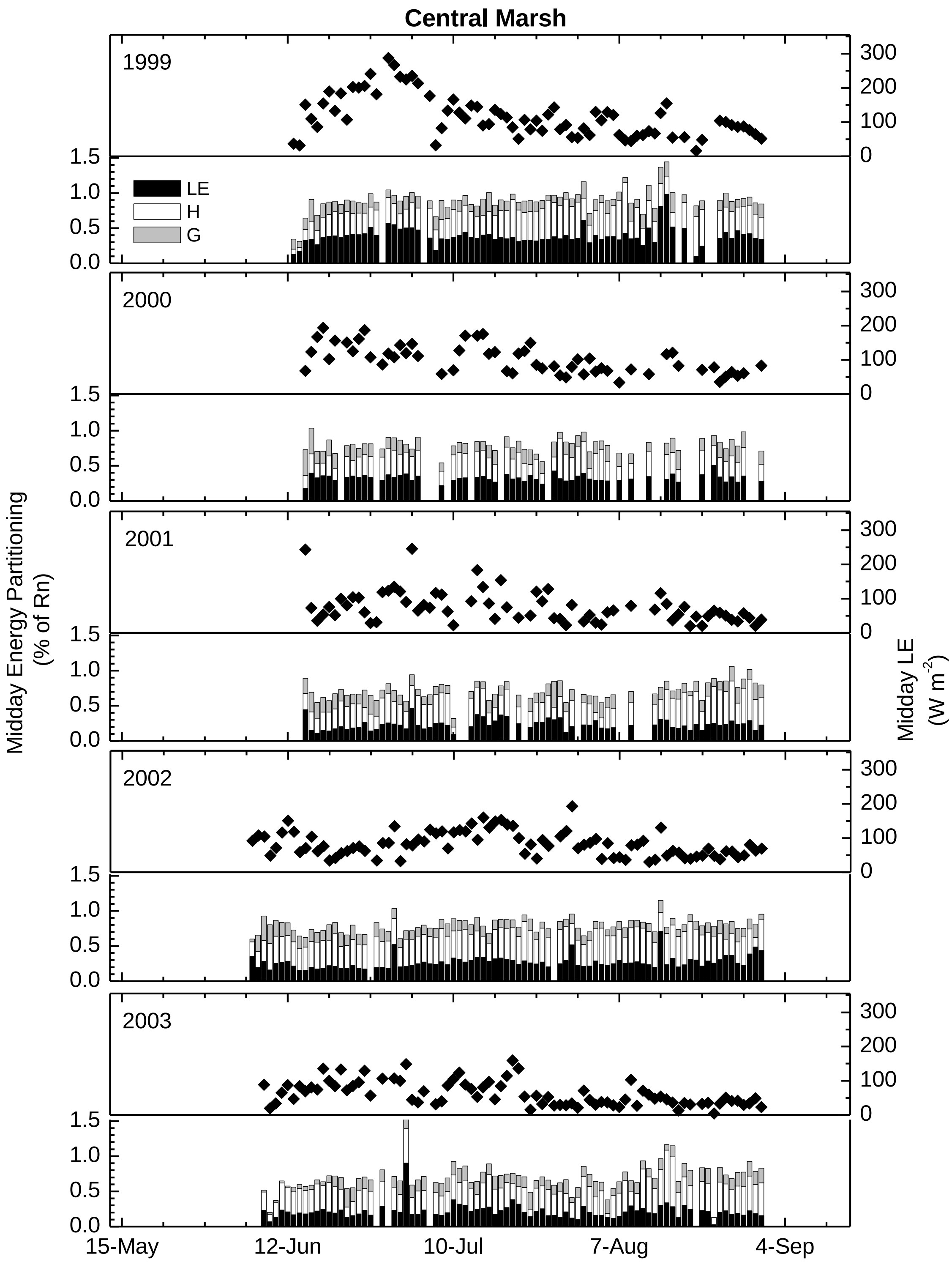

Central Marsh
1999
2000
2001
2002
2003
LE
H
G
Midday Energy Partitioning
(% of Rn)
Midday LE
(W m^{-2})
0.0
0.5
1.0
1.5
0
100
200
300
15-May
12-Jun
10-Jul
7-Aug
4-Sep

FIGURE 3b

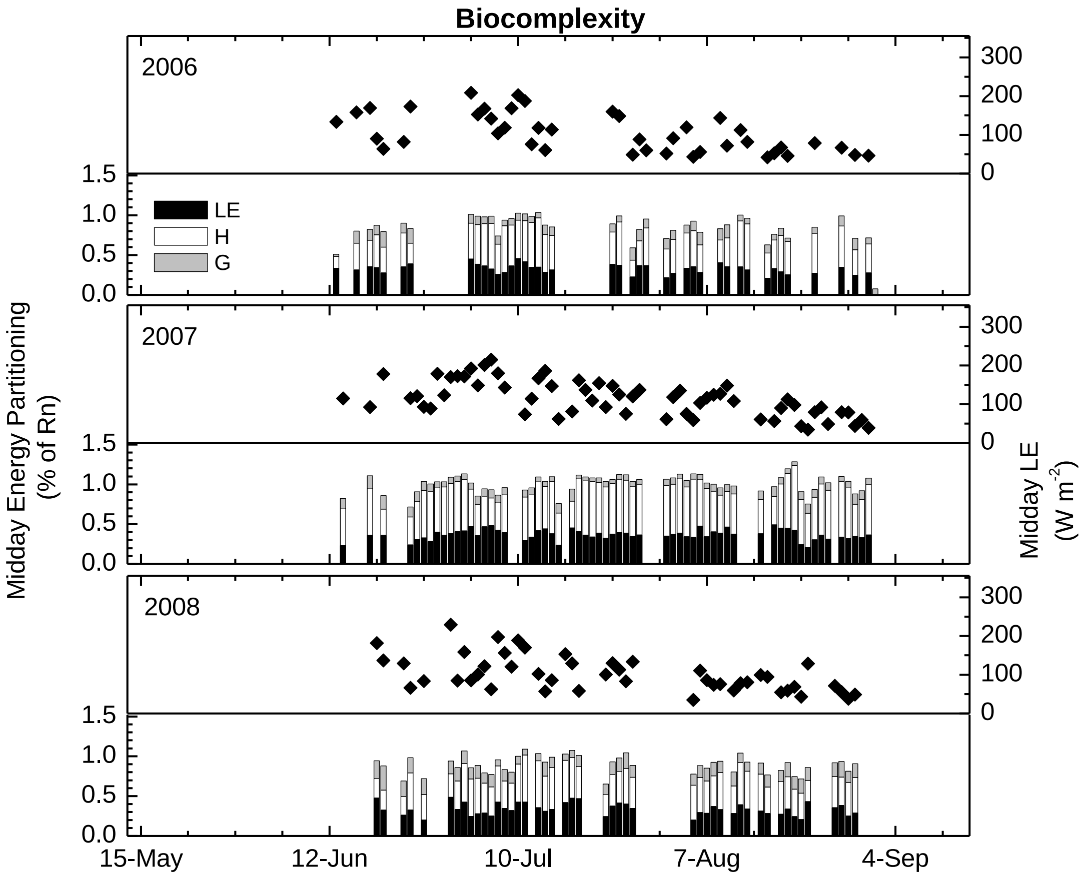
Biocomplexity
2006
2007
2008
LE
H
G
Midday Energy Partitioning (% of Rn)
Midday LE ($W m^{-2}$)
0.0
0.5
1.0
1.5
0
100
200
300
15-May
12-Jun
10-Jul
7-Aug
4-Sep

FIGURE 4

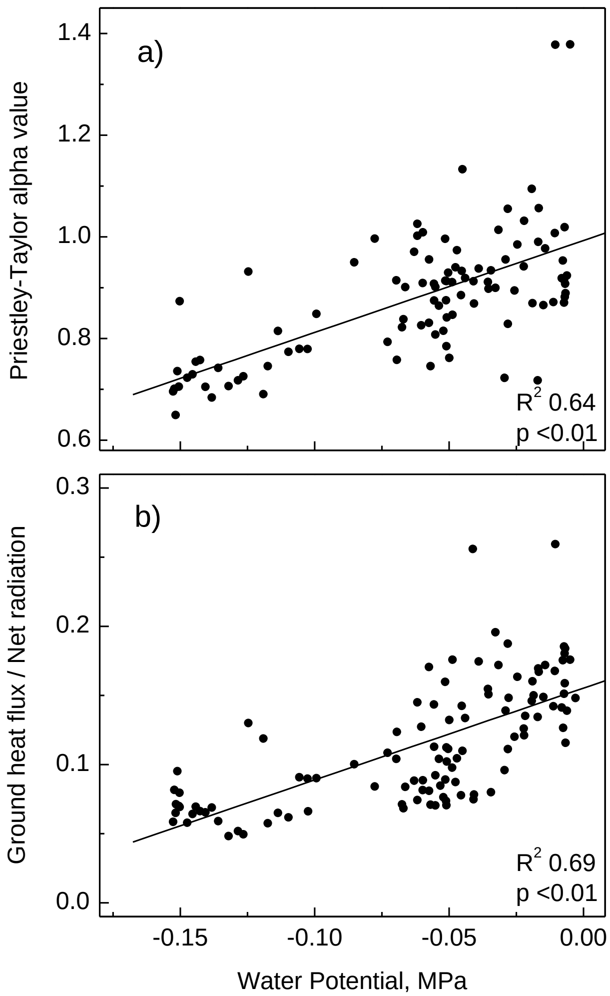
a)
Priestley-Taylor alpha value
1.4
1.2
1.0
0.8
0.6
R2 0.64
p <0.01
b)
Ground heat flux / Net radiation
0.3
0.2
0.1
0.0
R2 0.69
p <0.01
-0.15
-0.10
-0.05
0.00
Water Potential, MPa

FIGURE 5

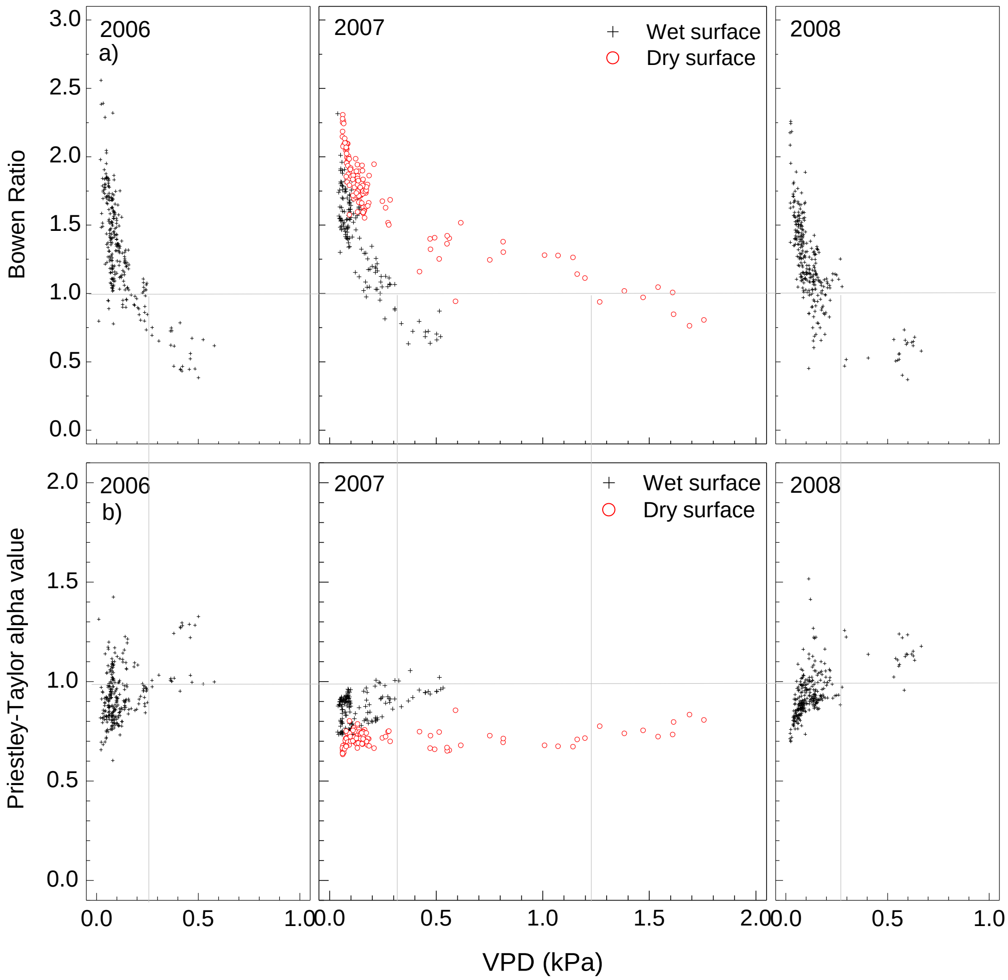

2006
a)
2007
Wet surface
Dry surface
2008
Bowen Ratio
2006
b)
2007
Wet surface
Dry surface
2008
Priestley-Taylor alpha value
VPD (kPa)

FIGURE 6

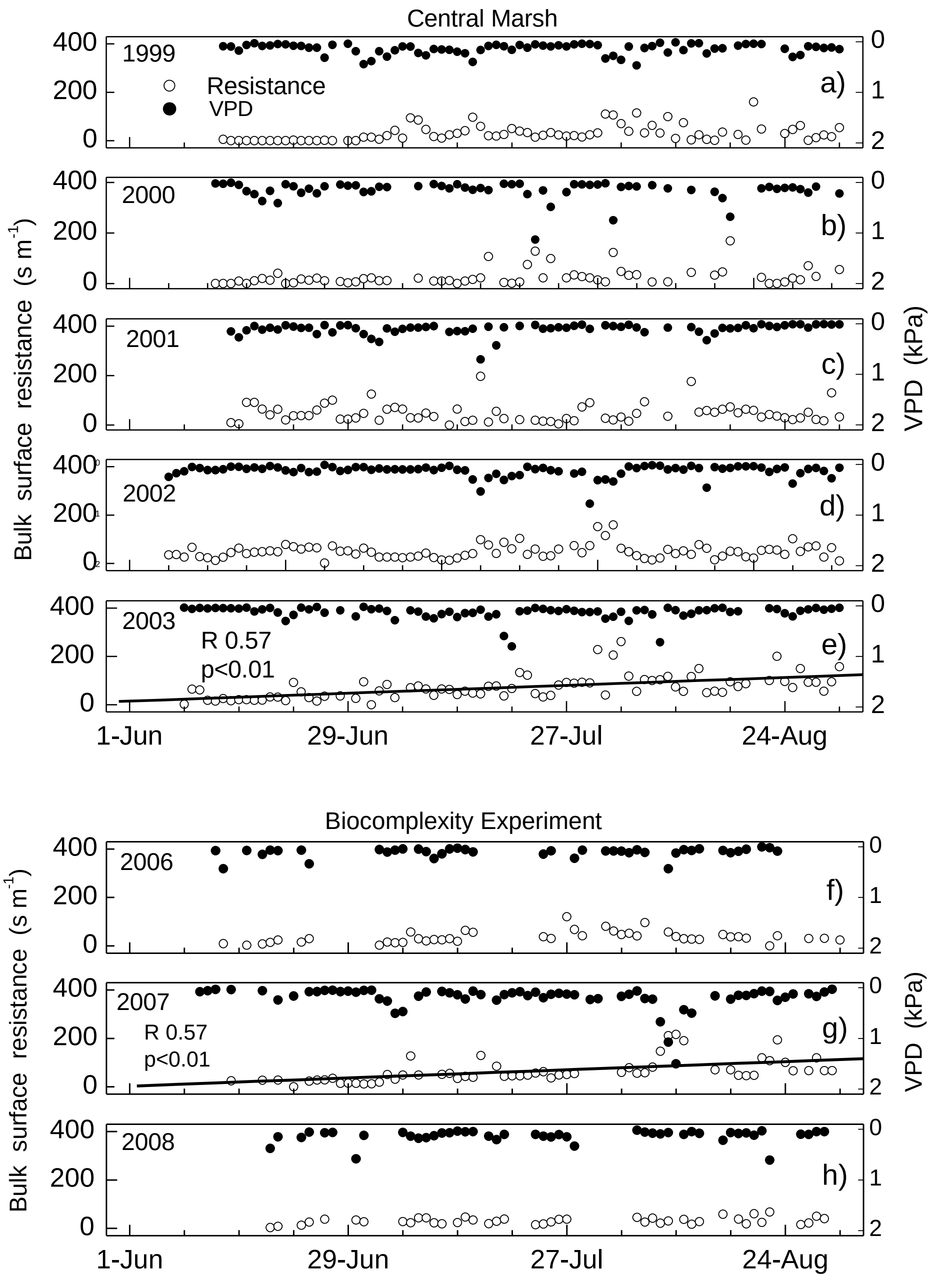
Central Marsh
Bulk surface resistance (s m-1)
VPD (kPa)
1999
2000
2001
2002
2003
Resistance
VPD
R 0.57
p<0.01
a)
b)
c)
d)
e)
1-Jun
29-Jun
27-Jul
24-Aug
Biocomplexity Experiment
2006
2007
2008
f)
g)
h)

FIGURE 7

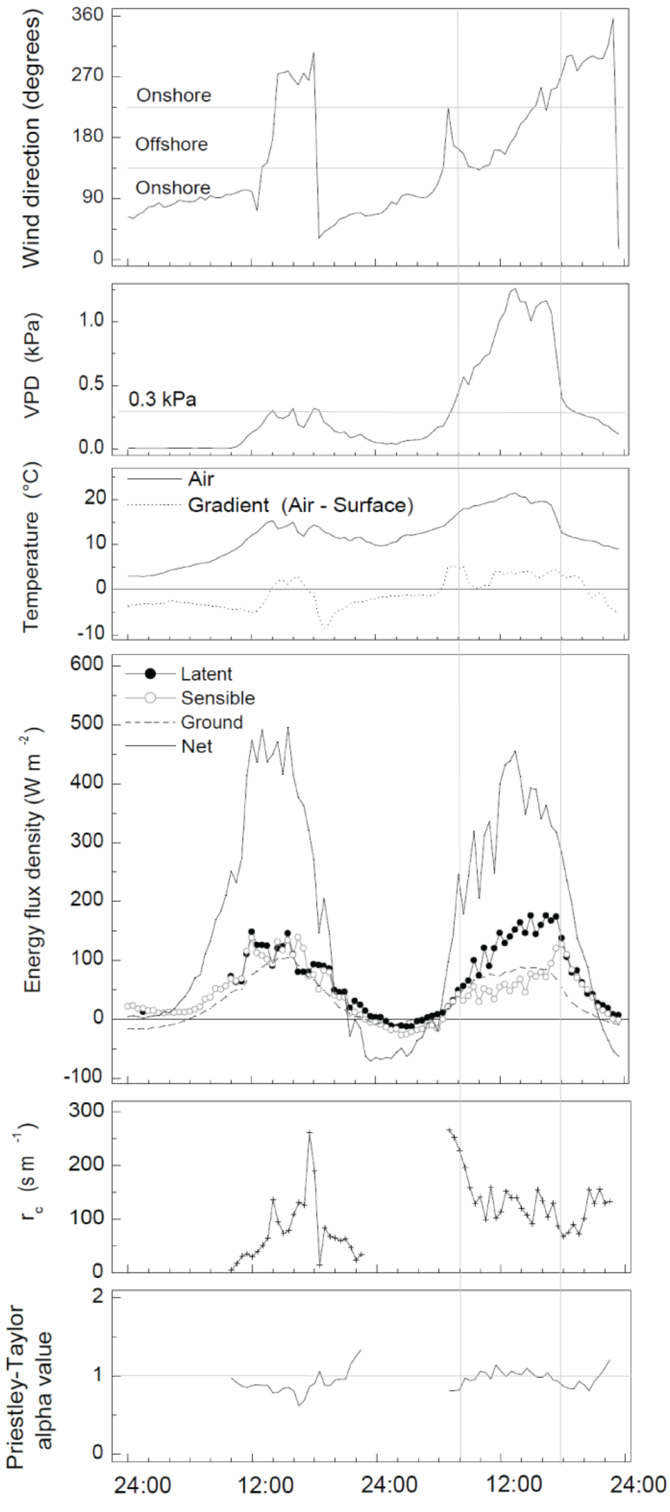

Wind direction (degrees)
360
270
180
90
0
Onshore
Offshore
Onshore
VPD (kPa)
1.0
0.5
0.0
0.3 kPa
Temperature (°C)
Air
Gradient (Air - Surface)
20
10
0
-10
Energy flux density (W m -2)
Latent
Sensible
Ground
Net
600
500
400
300
200
100
0
-100
r c (s m -1)
300
200
100
0
Priestley-Taylor alpha value
2
1
0
24:00
12:00
24:00
12:00
24:00